NEOPLASMA accepted, ahead of print manuscript
Cite article as https://doi.org/10.4149/neo_2026_251230N536

Running title: hnRNPD promotes the proliferation of Wilms' tumor cells

RNA-binding protein hnRNPD promotes the proliferation of Wilms' tumor cells through activating the p38 MAPK signaling pathway

Chunlei Yang[1,#], Man Liao[2,#], Haibin Bao[3], Haolun Xu[1], Jun Wang[1], Man Zhang[3], Can Li[3], Tian Zheng[4,*], Gang Li[3,*]

[1]Department of Urology, Wuhan Children's Hospital, Tongji Medical College, Huazhong University of Science and Technology, Wuhan, China; [2]Women's Health Section, Wuhan Children's Hospital, Tongji Medical College, Huazhong University of Science and Technology, Wuhan, China; [3]Department of General Surgery II (West Campus), Wuhan Children's Hospital, Tongji Medical College, Huazhong University of Science and Technology, Wuhan, China; [4]Department of Ophthalmology, Zhongnan Hospital of Wuhan University, Wuhan, China

***Correspondence:** znyyzt@163.com; wheylg@163.com

[#]Contributed equally to this work.

Received December 30, 2025 / Accepted July 27, 2026

Wilms' tumor (WT) represents a kidney carcinoma predominantly affecting children aged five years and younger. Heterogeneous nuclear ribonucleoprotein D (hnRNPD), an RNA-binding protein, has been implicated in oncogenic processes across various tumor types, whereas its expression pattern and biological function in WT remain largely unknown. hnRNPD expression within WT tissues was evaluated using publicly available databases, and co-expressed genes were identified through bioinformatic analysis. *In vitro*, hnRNPD expression in WT cell lines 17.94 and HFWT was modulated via gene silencing or overexpression. We subsequently carried out functional assays to assess cell proliferation and apoptosis. Molecular experiments were conducted to determine p38 mitogen-activated protein kinase (p38 MAPK) pathway activation status within cells with altered hnRNPD expression. Furthermore, SB203580 was utilized to pharmacologically inhibit this pathway to investigate the mechanism of hnRNPD in regulating WT cell proliferation.

Data showed that hnRNPD was upregulated in WT tissues and cells. Silencing hnRNPD significantly inhibited WT cell proliferation and promoted apoptosis. Conversely, overexpression of hnRNPD produced the opposing effects. MAPK14, the gene encoding the p38α isoform of p38 MAPK, was identified as a core gene within the hnRNPD co-expression network. Furthermore, the phosphorylation level of p38 MAPK in WT cells was markedly elevated compared to that in normal cells. However, inhibition of the p38 MAPK pathway using SB203580 suppressed WT cell proliferation. Notably, SB203580 effectively counteracted the pro-proliferative effect of hnRNPD overexpression on malignant WT cell growth.

In conclusion, hnRNPD is highly expressed in WT and plays a significant role in promoting the malignant proliferation of WT cells. The underlying molecular mechanism involves the regulation of p38 MAPK signaling pathway activation.

Key words: Wilms' tumor; heterogeneous nuclear ribonucleoprotein D; cell proliferation; p38 mitogen-activated protein kinase

Nephroblastoma, called Wilms' tumor (WT) as well, is a frequently seen pediatric renal cancer and is exceedingly rare in adults [1, 2]. As surgical treatment, radiotherapy and chemotherapy are used in combination, its five-year survival rate for early-stage children having favorable histology exceeds 90% [3, 4]. However, the prognosis for high-risk patients such as those with diffuse anaplastic histology, metastatic blastemal-type disease, or multiple recurrences remains poor [5]. Currently, significant challenges remain in the individualized treatment, prognosis assessment for specific patient subgroups, and long-term quality of life management in WT therapy. However, with advances in molecular biology and precision medicine, targeted therapies have demonstrated considerable potential and are increasingly regarded as a pivotal strategy for addressing current limitations in WT management [6]. Therefore, a more comprehensive understanding of the pathogenesis of WT is essential to identify novel therapeutic targets and advance the development of targeted interventions.

It is widely recognized that RNA-binding proteins (RBPs) serve as critical regulators of cellular processes and function as key coordinators in the post-transcriptional phase of the "central dogma" of gene expression. They are involved in essential steps including RNA processing, modification, nuclear- cytoplasmic transport, translation, and degradation [7, 8]. Aberrant expression of numerous RBPs has been observed in various cancers, where they contribute to tumorigenesis, invasion, and metastasis through the regulation of proto-oncogene or tumor suppressor gene mRNAs [9, 10]. Heterogeneous nuclear ribonucleoprotein D (hnRNPD), also known as AU-rich element RNA-binding factor 1 (AUF1), is a multifunctional RBP that belongs to the heterogeneous nuclear ribonucleoprotein (hnRNP) family and plays a central role in the post-transcriptional regulation of gene expression. hnRNPD specifically binds to AU-rich elements (AREs) located within the 3'-untranslated region (3'-UTR) of target mRNAs, thereby modulating the stability of these transcripts [11]. hnRNPD is aberrantly expressed in various types of tumors, including breast cancer [12], lung cancer [13], gastric cancer [14], and colorectal cancer [15], where it promotes tumorigenesis by enhancing the stability of proto-oncogenes or disrupting tumor suppressor genes. Nonetheless, its expression pattern and function in WT are largely unknown.

The mitogen-activated protein kinase (MAPK) signaling pathway is a highly conserved signaling cascade that plays a central role in regulating cellular proliferation, growth, survival, and stress adaptation. Aberrant activation of this pathway has been widely implicated in tumor initiation and progression across multiple cancer types, making MAPK signaling an important therapeutic target in oncology [16-18]. Emerging evidence suggests that dysregulated MAPK signaling contributes to the pathogenesis of WT [19]. In addition to its established roles in renal development, aberrant MAPK/ERK activation has been implicated in WT tumorigenesis, while activation of MAPK

signaling has also been shown to enhance NK cell-mediated antitumor immunity in WT, highlighting the multifaceted role of this pathway in WT biology [19, 20]. Among the MAPK family members, p38 MAPK has emerged as a critical regulator of tumor cell proliferation and progression. Aberrant activation of p38 MAPK signaling has been associated with enhanced tumor growth, invasion, metastasis, and therapeutic resistance in multiple malignancies, although its biological functions may vary depending on tumor type and cellular context [21, 22]. However, its biological role and upstream regulatory mechanisms in WT remain poorly understood. Given the post-transcriptional regulatory function of hnRNPD and the potential involvement of p38 MAPK signaling in WT, whether hnRNPD contributes to WT progression through modulation of the p38 MAPK pathway warrants further investigation.

Based on these observations, we hypothesized that hnRNPD promotes WT progression through activation of the p38 MAPK signaling pathway. Accordingly, the present study aimed to investigate the expression pattern and biological function of hnRNPD in WT and to determine whether its oncogenic effects are mediated by p38 MAPK signaling. To address this question, we combined bioinformatics analyses with *in vitro* gain- and loss-of-function experiments to characterize the role of hnRNPD in WT progression and to explore its underlying molecular mechanism, with the ultimate goal of identifying potential therapeutic targets for WT.

Patients and methods

Clinical specimens. Twelve paired WT tissues and adjacent normal kidney tissues were collected from patients who underwent surgical resection at Wuhan Children's Hospital between January 2024 and March 2026. All tissue specimens were histopathologically confirmed by two experienced pathologists. This study was approved by the Ethics Committee of Wuhan Children's Hospital (Approval No. 2025R130-E01), and written informed consent was obtained from the legal guardians of all patients. Clinical information, including age, sex, NWTS-5 stage, and TNM stage, was collected for all enrolled patients.

Bioinformatics analysis. RNA-Seq data associated with WT (TARGET-WT) were obtained from the Genomic Data Commons (GDC) Data portal (https://portal.gdc.cancer.gov/), comprising 130 tumors alongside 6 non-carcinoma tissues. Additionally, the GSE138869 dataset related to WT was acquired in GEO database (https://www.ncbi.nlm.nih.gov/geo/), comprising 5 tumors as well as 5 normal tissue samples. Box plots were generated using R packages such as ggplot2, and the differential expression of hnRNPD in WT versus non-carcinoma samples was evaluated using Wilcoxon rank-sum test. Besides, we utilized R ggpubr package for analyzing hnRNPD expression-related genes in TARGET-WT dataset, with the correlation coefficient being $r \geq 0.5$ and

statistical significance being $p < 0.05$. The identified associated genes were utilized for constructing the co-expression network using Cytoscape, while CytoNCA plugin was employed to calculate centrality scores for the network nodes, thereby screening out the core genes.

Cell culture and transfection. WT cells (17.94 and HFWT) were provided by Deutsche Sammlung von Mikroorganismen und Zellkulture (DSMZ, Braunschweig, Germany) and Cell Bank of RIKEN BioResource Research Center (Tsukubashi, Japan), respectively. Meanwhile, human renal proximal tubular epithelial cells (HK-2) were acquired in Cell Bank of the Committee on Type Culture Collection, Chinese Academy of Sciences. The 17.94 cells were cultivated within Dulbecco's Modified Eagle Medium (DMEM) (Gibco, Carlsbad, USA) that contained 20% fetal bovine serum (FBS) (Gibco, Carlsbad, USA), HFWT cells within Ham's F-12 medium (Procell, Wuhan, China) containing 15% FBS, and the HK-2 cells within Keratinocyte-SFM medium (Gibco, Carlsbad, USA).

The transcript sequence NM_031370.3 of *hnRNPD* was retrieved from the NCBI database (https://www.ncbi.nlm.nih.gov/), and the corresponding coding sequence (CDS) was cloned into the pcDNA3.1(+) expression vector (GenePharma, Shanghai, China) to generate an hnRNPD overexpression construct. Based on the CDS sequence, potential interference sequences were designed using the online tool DSIR (http://biodev.extra.cea.fr/DSIR/DSIR.html). The candidate siRNA sequences were subsequently subjected to BLAST analysis to ensure specificity, and three siRNAs with high specificity for the target gene were selected for the construction of *hnRNPD* RNA interference plasmids (GenePharma, Shanghai, China). Both the overexpression and interference plasmids were transfected into 17.94 and HFWT cells using Lipofectamine 3000 (Invitrogen, Carlsbad, USA). Following 48 h of transfection, cells were harvested for quantitative real-time PCR (qRT-PCR) and Western blot analyses to validate expression levels of hnRNPD. The siRNA sequences are as follows:si-hnRNPD-1#: 5'-GAACCAGUGAAGAAGAUAAUG-3' and 5'-UUAUCU UCUUCACUGGUUCUU-3'; si-hnRNPD-2#: 5'-GCUGGGACACUACAAAGAAA G-3' and 5'-UUCUUUGUAGUGUCCCAGCUA-3'; si-hnRNPD-3#: 5'-CCAUGGA CAACAAGACCAAU A-3' and 5'-UUGGUCUUGUUGUCCAU GGGG-3'.

Cell counting kit-8 (CCK-8) assay. The collected 17.94 and HFWT cells were inoculated into 96-well plates at 3×10^3 cells/well. Following cell adhesion, the cultures were maintained for 12, 24, 48, or 72 h, respectively. In parallel experiments, cells underwent 24 h of treatment using p38 MAPK pathway inhibitor SB203580 (10 μM, Selleck, Houston, USA) [23]. Subsequently, CCK-8 solution (10 μl, Solabio, Beijing, China) was introduced into every well for 2 h of incubation. Thereafter, all plates were removed from the incubator, and absorbance (OD) values were determined at 450 nm using the microplate reader.

5-Ethynyl-2'-deoxyuridine (EdU) staining. Both WT cell lines were inoculated in the 12-well plates for overnight culture. Following a 24 h treatment with or without SB203580, an equal volume of 20 μM EdU-488 working solution (Servicebio, Wuhan, China) was introduced into culture medium for 2 h of incubation. After removing supernatants, cells were subjected to 15 min of fixation with 4% paraformaldehyde, followed by permeabilization using permeabilization solution for 10 min. The EdU reaction mixture was prepared following specific protocols and applied to cells for a 30 min incubation period. Following Hoechst 33342 staining of cell nuclei, EdU-positive cells exhibiting green fluorescence were observed in five non-overlapping fields of view for each sample under the fluorescence microscope. Both EdU-positive cell and total cell numbers within these fields were quantified with ImageJ software.

Flow cytometry analyses. For the assessment of apoptosis rate, cells were harvested, counted, and 1×10^6 cells per sample were collected. The cells were washed twice with phosphate-buffered saline (PBS), and resuspended in 100 μl of Binding Buffer, followed by the sequential addition of 5 μl of Annexin V-FITC and 5 μl of Propidium Iodide (PI) (Servicebio, Wuhan, China). After gentle mixing, the samples were incubated in the dark for 15 min. Subsequently, 400 μl of Binding Buffer was added to each sample, and the apoptosis rate was analyzed using a flow cytometer. For cell cycle analysis, cells were harvested, counted, and 1×10^6 cells per sample were collected. After washing twice with PBS, the cells were fixed in 70% cold ethanol at 4 °C overnight. The fixed cells were washed with PBS and incubated with PI/RNase A staining solution (Servicebio, Wuhan, China) in the dark for 30 min at room temperature. Cell cycle distribution was subsequently analyzed using a flow cytometer.

qRT-PCR analysis. One milliliter of TRIzol reagent (Invitrogen, Carlsbad, USA) was added to 1×10^6 cells to facilitate cell lysis and total RNA extraction. For clinical validation, total RNA was also extracted from paired WT tissues and adjacent normal kidney tissues using the same TRIzol-based protocol. The extracted RNA quantity and quality were subsequently evaluated. Then, RNA (1 μg) served as template, with the addition of 10 μM forward primer and reverse primer. The SuperScript™ III Platinum™ one-step qRT-PCR kit (Invitrogen, Carlsbad, USA) was adopted to conduct reverse transcription and quantitative PCR upon thermal cycling conditions below: 15 min cDNA synthesis under 50 °C; 2 min initial denaturation under 95 °C; 15 s denaturation under 95 °C alongside 30 s annealing/extension under 60 °C for 40 cycles. *hnRNPD* mRNA level in both cultured cells and clinical tissue specimens was determined by the $2^{-\Delta\Delta Ct}$ approach, and *TUBB1* was an endogenous control gene. Primer sequences were shown below: *hnRNPD* forward: 5'-GGAAGAGCTCGTGGA AGAGG-3' and reverse: 5'-AACCACTCTGCTGGTTGCTA-3'; *TUBB1* forward: 5'-ATTCCAACCTTCCAGCCTGC-3' and reverse:

5’-ATCACCTCCCAGAACTTG GC -3’.

Western blotting. RIPA lysis buffer (Beyotime, Shanghai, China) was introduced into cells and later this mixture was shaken repeatedly to ensure thorough mixing. For clinical specimen validation, total protein was also extracted from paired WT tissues and adjacent normal kidney tissues using the same RIPA lysis protocol. After 30 min of lysis on ice, the total protein solution was obtained. After determining concentration, the protein samples were loaded onto the gel for electrophoresis separation before transfer on polyvinylidene fluoride (PVDF) membranes (Millipore, Billerica, USA), which were subsequently immersed in 5% skim milk solution for a 2 h duration under ambient temperature. Subsequently, membranes were incubated overnight primary antibody incubation under 4 °C and later secondary antibody probing for a 50 min period under ambient temperature. The rinsed membranes were incubated, chemiluminescence reagent was added, reacted for 1 min, and exposed. Finally, protein band intensities were measured with Image J, while target protein levels were calculated based on β-Tubulin. The expression level of hnRNPD protein was further examined in clinical tissue specimens using the same Western blot procedure. All rabbit-derived primary antibodies used in the Western blot experiments were obtained from Cell Signaling Technology (Danvers, USA) or Abcam (Cambridge, UK) and applied at a dilution ratio of 1:1000. The antibodies targeted hnRNPD (#12382), p38 MAPK (#9212), p-p38 MAPK (Thr180/Try182) (#9211), ATF-2(ab239361), phospho-ATF-2 (Thr69/71) (ab32019), proliferating cell nuclear antigen (PCNA) (#13110), Cyclin D1 (#2922), Cleaved Caspase-3 (#9664), and β-Tubulin (#2128), respectively.

Statistical analysis. All experiments in this study were carried out with three biological replicates. GraphPad Prism 8 was adopted for implementing statistical analysis. Two-group comparisons used unpaired t-tests; multi-group differences were examined through one-way ANOVA plus Tukey’s post hoc test. The associations between hnRNPD expression and clinicopathological variables were evaluated using Fisher's exact test. P-value < 0.05 stood for significant differences.

Results

hnRNPD is highly expressed in WT. Based on an analysis of hnRNPD expression levels in WT using public databases (TARGET-WT and GSE138869), we observed that hnRNPD was significantly upregulated in WT tissues (Figure 1A). However, the clinical information for WT patients in the TARGET-WT dataset is severely limited, lacking many key clinicopathological parameters and prognostic data. This may be attributed to the fact that the TARGET-WT dataset primarily encompasses common and highly lethal adult malignant tumors, and WT is among its peripheral items. Consequently, we were unable to further analyze the relationship between the

expression level of hnRNPD and the clinicopathological parameters or prognosis of WT patients. Meanwhile, we also observed that hnRNPD was significantly upregulated in WT cell lines (Figures 1B, 1C). Therefore, the abnormal expression of hnRNPD may be involved in the malignant process of WT. To further validate the results obtained from the analysis of the public database, this study conducted RT-qPCR and Western blot analyses using 12 pairs of WT tissue and adjacent normal kidney tissue samples. The RT-qPCR results indicated that the expression levels of hnRNPD mRNA were significantly higher in WT tissues than in adjacent normal tissues. The Western blot analysis further verified that the expression of hnRNPD protein was markedly increased in tumor tissues compared to adjacent normal tissues. These findings are in line with the results from the public database analysis, jointly confirming that hnRNPD is abnormally overexpressed in WT tissues (Supplementary Figure S1). To further assess the clinical relevance of hnRNPD, the 12 WT samples were divided into high- and low-expression groups based on the median hnRNPD expression level. Clinicopathological analysis showed that high hnRNPD expression was significantly associated with advanced NWTS-5 clinicopathological stage ($p=0.023$), whereas no significant associations were observed with age, sex, or TNM stage (Supplementary Table S1).

Silencing hnRNPD suppresses WT cell proliferation and promotes apoptosis. For investigating biological roles of hnRNPD in the malignant progression of WT, we conducted RNA interference for specifically silencing hnRNPD within WT cells. Based on qRT-PCR and Western blot analyses, the si-hnRNPD-3# with greatest knockdown efficiency was chosen to conduct later transfection assays (Figure 2). In subsequent functional tests, it was discovered that the silencing of hnRNPD decreased the 17.94 and HFWT cell viability and cell proliferation (Figures 3A, 3B). The results demonstrated that the silencing of hnRNPD led to a significant increase in the proportion of cells in the G0/G1 phase, accompanied by a notable decrease in the proportions of cells in the S and G2/M phases, which indicates an arrest in the G1 phase. Conversely, the overexpression of hnRNPD resulted in a reduction in the proportion of G0/G1 phase cells and an increase in those in the S and G2/M phases. This suggests that hnRNPD facilitates the G1/S transition and expedites the entry into DNA replication, thereby further corroborating the conclusion that hnRNPD enhances the proliferation of WT cells (Supplementary Figure S2). Conversely, the apoptosis rates of 17.94 and HFWT cells exhibited a substantial increase subsequent to hnRNPD knockdown (Figure 3C). Moreover, it was observed that the silencing of hnRNPD down-regulated the protein expression levels of PCNA and Cyclin D1 in 17.94 and HFWT cells, while concurrently increasing the expression level of the pro-apoptotic protein Cleaved Caspase-3 (Figure 3D). Collectively, these findings suggest that hnRNPD plays a critical regulatory role in the proliferation and apoptosis of WT cells. Knockdown of hnRNPD can effectively suppress WT cells proliferation and promote cell

apoptosis.

Silencing hnRNPD inhibits the p38 signaling pathway activation within WT cells. For investigating the potential mechanism through which hnRNPD influences WT cell proliferation and apoptosis, this study conducted an analysis of its associated genes. In the TARGET-WT dataset, 241 genes were identified as being co-expressed with hnRNPD (Figure 4A). The complete lists of positively and negatively co-expressed genes with hnRNPD are provided in Supplementary Table S2. A co-expression network was constructed, and centrality scoring was applied to identify hub nodes, leading to the selection of 17 core genes (Figure 4B). Detailed CytoNCA scores of all candidate genes are presented in Supplementary Table S3. Among these, *MAPK14* encoding the p38α isoform of p38 MAPK was recognized as a central hub gene due to its high connectivity with other core genes. Given its pivotal regulatory role within the network, p38 MAPK was selected as the primary target for further investigation into the underlying molecular mechanisms. Furthermore, the phosphorylation levels at the Thr180/Tyr182 residues of p38 MAPK in WT cells were significantly higher than those observed in HK-2 cells. However, silencing of hnRNPD suppressed the phosphorylation of the Thr180/Tyr182 residues in p38 MAPK in WT cells (Figure 4C). Therefore, we hypothesize that hnRNPD may play a critical regulatory role in the malignant proliferation of WT cells by promoting p38 MAPK activation.

Inhibition of the p38 MAPK signaling pathway effectively reverses the hnRNPD- mediated promotion of the malignant proliferation in WT cells. To validate the aforementioned hypothesis, we overexpressed hnRNPD in WT cells (Figures 5A, 5B) and subsequently treated the cells with SB203580, a specific inhibitor of the p38 MAPK signaling pathway. The results, as shown in Supplementary Figure S3, indicated that, when compared with the Vector group, the overexpression of hnRNPD significantly enhanced the proliferation capacity of 17.94 and HFWT cells. Moreover, this promoting effect gradually increased as the culture time was prolonged, which further confirmed the role of hnRNPD in promoting WT cell proliferation. Treatment with SB203580 alone significantly reduced the viability of 17.94 and HFWT cells and suppressed their proliferative capacity. In contrast, hnRNPD overexpression exerted a protective effect, enhancing cell viability and increasing the number of proliferating cells (Figures 5C, 5D). Furthermore, SB203580 treatment markedly increased the apoptosis rate in both 17.94 and HFWT cells, whereas upregulation of hnRNPD expression effectively attenuated apoptosis in WT cells (Figure 6A). Moreover, overexpression of hnRNPD markedly upregulated the expression levels of PCNA and Cyclin D1 while downregulating that of Cleaved Caspase-3. In contrast, treatment with SB203580 reduced the expression of PCNA and Cyclin D1 and enhanced the expression of Cleaved Caspase-3 (Figure 6B). Notably, co-treatment with SB203580 effectively reversed the effects of hnRNPD

overexpression on malignant proliferation, apoptosis, and associated protein expression in WT cells. These findings indicate that hnRNPD promotes malignant proliferation in WT cells through modulation of the p38 MAPK signaling pathway. To further assess the activation status of the p38 MAPK signaling pathway, we investigated the expression levels of total p38 (p38 MAPK), phosphorylated p38 (p-p38 MAPK), and their typical downstream target protein ATF-2 and phosphorylated ATF-2 (p-ATF-2). Subsequently, we conducted a quantitative analysis of the ratios of p-p38 MAPK/p38 MAPK and p-ATF-2/ATF-2. Western blot results (Supplementary Figure S4) indicated that, in comparison with the Vector group, the overexpression of hnRNPD notably enhanced the p-p38 MAPK/p38 MAPK ratio in WT cells and facilitated an increase in the phosphorylation of ATF-2, whereas the expression of total p38 and total ATF-2 proteins remained substantially unchanged. Further treatment with SB203580 resulted in a significant reduction in both the p-p38 MAPK/p38 MAPK and p-ATF-2/ATF-2 ratios and significantly inhibited the activation of the signal pathway induced by hnRNPD overexpression. These findings further corroborate that hnRNPD promotes the activation of the p38 MAPK signaling pathway and the downstream ATF-2 transcriptional activity in WT cells, and that SB203580 effectively impedes this process.

Discussion

Currently, the management of WT following diagnosis primarily involves conventional surgical intervention, supplemented by postoperative radiotherapy and chemotherapy. Although conventional treatment approaches can enhance patient survival rates to some extent, surgical trauma and long-term adverse effects may significantly impair patients' quality of life [24]. Therefore, the exploration of targeted intervention strategies for WT has emerged as a prominent research focus in this field. This study represents the investigation into the expression, functional role, and potential molecular mechanisms of hnRNPD in WT, identifying hnRNPD as a promising therapeutic target for this malignancy. Bioinformatics analyses demonstrated that hnRNPD is significantly upregulated in WT tissues, a finding consistently corroborated at the cellular level. *In vitro* functional assays further revealed that silencing hnRNPD markedly suppresses malignant proliferation in WT cells. Mechanistically, the oncogenic activity of hnRNPD in WT may be associated with its modulation of p38 MAPK signaling pathway activity.

hnRNPD is an RNA-binding protein involved in the regulation of mRNA stability, splicing, transport, and translation [25]. Its elevated expression can remodel the cellular transcriptome by modulating the transcripts of multiple downstream oncogenes and tumor suppressor genes, thereby promoting tumorigenesis. Recent research findings have demonstrated that hnRNPD is highly

expressed in gastric cancer and promotes the proliferation of gastric cancer cells through direct regulation of thioredoxin- interacting protein (TXNIP) [14]. hnRNPD is also overexpressed in glioma tissues and cell lines, where it enhances the transcription of angiogenesis-related proteins—including MMP2, MMP9, and VE-cadherin via modulation of the linc00707/ miR-651-3p/SP2 signaling axis, thereby facilitating glioma angiogenesis [26]. In colorectal cancer, hnRNPD binds to the AREs within the 3'-UTR of the downstream target gene RBM47, leading to transcript destabilization and subsequent suppression of the p53 signaling pathway in gastric cancer cells, thereby promoting colorectal cancer cell proliferation and metastasis [27]. We found that hnRNPD was abnormally highly expressed in WT tissues and cells. Considering its established oncogenic role in various tumor types, we hypothesize that elevated hnRNPD expression may contribute to a permissive intracellular environment conducive to WT progression. Our findings demonstrate that silencing hnRNPD suppresses malignant proliferation in WT cells, indicating that hnRNPD plays a critical role in regulating the survival and proliferation of WT. Silencing hnRNPD primarily exerts an inhibitory effect on the proliferation of WT cells through the following mechanisms: down-regulating the cell proliferation related protein PCNA, which directly inhibits cell proliferation; down-regulating the cell cycle regulatory protein Cyclin D1, which disrupts the cell-cycle operation and consequently impedes cell proliferation; and promoting the expression of the apoptosis effector Cleaved Caspase-3, thereby accelerating cell death. In contrast, overexpression of hnRNPD has the opposite effects on the proliferation and apoptosis of WT cells. Report has indicated that sarcomas develop in transgenic mice overexpressing hnRNPD, with significantly upregulated expression of Cyclin D1 observed in tumor tissues [28]. Furthermore, AREs are present in the 3'-UTR of Cyclin D1 mRNA [29], suggesting a potential direct regulatory role of hnRNPD in modulating Cyclin D1 expression. Collectively, our findings demonstrate that hnRNPD promotes malignant proliferation of WT cells and exerts oncogenic effects.

Based on the TARGET-WT dataset, correlation analysis revealed that MAPK14, which encodes the p38α isoform of p38 MAPK, is a central node in the co-expression network of hnRNPD. The expression of phosphorylated p38 MAPK was elevated in WT cells. Furthermore, knockdown of hnRNPD suppressed p38 MAPK phosphorylation within WT cells, whereas overexpression of hnRNPD enhanced p38 MAPK pathway activation. As indicated by these findings, the p38 MAPK signaling pathway probably serves as the potential mechanism through which hnRNPD accelerates WT progression. The dual role of the p38 MAPK pathway in tumorigenesis renders it a highly promising but complex therapeutic target. Study has shown that senescent cells contribute to skin carcinogenesis through upregulation of the p38 MAPK signaling pathway [30]. Inhibition of this pathway has been shown to suppress migration and invasion of breast cancer cells, thereby

attenuating tumor progression and lung metastasis [31]. Bone morphogenetic protein 9 (BMP9) exerts pro-tumorigenic effects in hepatocellular carcinoma (HCC), with its protective role in HCC cell survival dependent on p38 MAPK activation20. Furthermore, dual inhibition of p38 MAPK and PIKfyve kinase have been demonstrated to significantly reduce the viability of multiple cancer cell types and to inhibit tumor growth in murine models of colorectal cancer xenografts [32]. The aforementioned research indicates that leveraging p38 MAPK's effect on promoting tumor occurrence and transforming it into a therapeutic target for specific cancer types holds significant potential for advancing tumor treatment. In this study, the application of SB203580 in suppressing this signaling pathway within WT cells markedly inhibited cell proliferation and induced apoptosis, suggesting that this pathway promotes WT progression. Notably, inhibiting this pathway abrogated the stimulatory effect of hnRNPD upregulation on the malignant proliferation of WT cells, indicating that hnRNPD may drive malignant cellular proliferation in WT through activating this pathway. It is noteworthy that, as an RNA-binding protein, hnRNPD predominantly exerts its biological functions through the regulation of the stability of target mRNAs rather than via direct interaction with signaling proteins. This study validates that hnRNPD can activate the p38 MAPK signaling pathway in WT cells; however, it remains to be determined whether it directly binds to MAPK14 mRNA. In view of our prior findings indicating that hnRNPD directly binds to and stabilizes MAP4K4 mRNA [33], and given that MAP4K4 functions as a crucial upstream kinase for p38 MAPK, it is more probable that hnRNPD indirectly activates the p38 MAPK pathway by augmenting the stability of MAP4K4 mRNA, rather than directly regulating MAPK14. This potential molecular mechanism necessitates further experimental verification.

The p38 MAPK signaling pathway demonstrates substantial tissue- and cell context-dependent effects, acting as either oncogenic or tumor-suppressive in diverse cancers. This research reveals that the overexpression of hnRNPD notably elevates the phosphorylation levels of p38 MAPK and its downstream effector ATF-2. Meanwhile, the p38 MAPK-specific inhibitor SB203580 significantly reverses the cell proliferation induced by hnRNPD, suggesting that the constitutively activated p38 MAPK predominantly promotes tumorigenesis in WT cells. In combination with the results of cell cycle analysis, the overexpression of hnRNPD facilitates the G1/S phase transition, while its silencing results in G1 phase arrest. This further implies that the activation of p38 MAPK mediated by hnRNPD may enhance the proliferation of WT cells by accelerating the cell cycle progression. Integrating these findings with prior research, we postulate that hnRNPD may stabilize MAP4K4 mRNA, thereby continuously activating the "MAP4K4–p38 MAPK" signaling axis and ultimately promoting the proliferation of WT cells and tumor progression. Although this regulatory mechanism necessitates further molecular studies for validation, this hypothesis provides a novel

theoretical foundation for comprehending the molecular mechanisms underlying the hnRNPD-driven malignant progression in WT, and offers new directions for exploring the regulation of MAPK signaling networks by RNA-binding proteins and developing potential targeted therapeutic strategies.

In conclusion, this study provides the first evidence that hnRNPD functions as an oncogenic RNA-binding protein in Wilms' tumor. Mechanistically, hnRNPD promotes WT cell proliferation, at least in part, through activation of the p38 MAPK signaling pathway. These findings broaden our understanding of WT pathogenesis and suggest that targeting the hnRNPD/p38 MAPK axis may represent a promising therapeutic strategy for WT.

However, this study has only preliminarily investigated certain biological functions of hnRNPD in WT and remains subject to several limitations: 1) although our previous work identified MAP4K4 as a direct downstream target of hnRNPD, whether hnRNPD directly regulates MAPK14 or other upstream components of the p38 MAPK pathway remains unclear; and 2) there is a lack of *in vivo* animal experimental data. To address these limitations, future studies will focus on the following aspects: 1) employing RIP-seq, CLIP-seq, and mRNA stability analyses to systematically characterize the RNA regulatory network of hnRNPD and further identify additional direct downstream targets involved in p38 MAPK signaling; and 2) establishing stable hnRNPD knockdown and overexpression WT cell lines, followed by tumor xenograft experiments in nude mice, to validate the oncogenic role of hnRNPD *in vivo*. Nevertheless, the integrated evidence from clinical specimens, *in vitro* functional assays, and mechanistic analyses consistently supports the conclusion that hnRNPD promotes WT cell proliferation through activation of the p38 MAPK signaling pathway, while *in vivo* validation will further strengthen the physiological relevance of these findings.

Acknowledgements: This work was financially supported by the General Project of Natural Science Foundation of Hubei Province (No. 2025AFB931).

Supplementary data are available in the online version of the paper.

References

[1] SERVAES SE, HOFFER FA, SMITH EA, KHANNA G. Imaging of Wilms tumor: an update. Pediatr Radiol 2019; 49: 1441-1452. https://doi.org/10.1007/s00247-019-04423-3

[2] CARAMANTI RL, APR GIO RM, DE MORAES DF, ROCHA C, MEGUINS LC et al. Brain Metastasis of Wilms Tumor in Adult. World Neurosurg 2020; 138: 422-424. https://doi.org/10.1016/j.wneu.2020.03.132

[3] BRISSE HJ, DE LA MONNERAYE Y, CARDOEN L, SCHLEIERMACHER G. From Wilms to kidney tumors: which ones require a biopsy? Pediatr Radiol 2020; 50: 1049-1051. https://doi.org/10.1007/s00247-020-04660-x

[4] BALIS F, GREEN DM, ANDERSON C, COOK S, DHILLON J et al. Wilms Tumor (Nephroblastoma), Version 2.2021, NCCN Clinical Practice Guidelines in Oncology. J Natl Compr Canc Netw 2021; 19: 945-977. https://doi.org/10.6004/jnccn.2021.0037

[5] ORTIZ MV, KOENIG C, ARMSTRONG AE, BROK J, DE CAMARGO B et al. Advances in the clinical management of high-risk Wilms tumors. Pediatr Blood Cancer 2023; 70: e30342. https://doi.org/10.1002/pbc.30342

[6] HONG B, DONG R. Research advances in the targeted therapy and immunotherapy of Wilms tumor: a narrative review. Transl Cancer Res 2021; 10: 1559-1567. https://doi.org/10.21037/tcr-20-3302

[7] GLISOVIC T, BACHORIK JL, YONG J, DREYFUSS G. RNA-binding proteins and post-transcriptional gene regulation. FEBS Lett 2008; 582: 1977-1986. https://doi.org/10.1016/j.febslet.2008.03.004

[8] ANJI A, KUMARI M. Guardian of Genetic Messenger-RNA-Binding Proteins. Biomolecules 2016; 6: 4. https://doi.org/10.3390/biom6010004

[9] QIN H, NI H, LIU Y, YUAN Y, XI T et al. RNA-binding proteins in tumor progression. J Hematol Oncol 2020; 13: 90. https://doi.org/10.1186/s13045-020-00927-w

[10] ZHANG Y, LI Z. RNA binding proteins: Linking mechanotransduction and tumor metastasis. Cancer Lett 2021; 496: 30-40. https://doi.org/10.1016/j.canlet.2020.09.020

[11] CUI H, LIU Z, PENG L, LIU L, XIE X et al. A novel 5'tRNA-derived fragment tRF-Tyr inhibits tumor progression by targeting hnRNPD in gastric cancer. Cell Commun Signal 2025; 23: 88. https://doi.org/10.1186/s12964-025-02086-2

[12] HU H, ZHANG H, XING Y, ZHOU Y, CHEN J et al. The lncRNA THOR interacts with and stabilizes hnRNPD to promote cell proliferation and metastasis in breast cancer. Oncogene 2022; 41: 5298-5314. https://doi.org/10.1038/s41388-022-02495-4

[13] ZHANG X, MENG P, WANG P, SONG Y. Activation of the SIRT1/PGC-1α pathway by HNRNPD promotes vasculogenic mimicry in NSCLC. Tissue Cell 2025; 95: 102903. https://doi.org/10.1016/j.tice.2025.102903

[14] ZOU X, LI J, ZHOU J, REN Q, WANG K et al. Silencing hnRNPD inhibits gastric cancer growth by increasing TXNIP-mediated oxidative stress. Discov Oncol 2025; 16: 798. https://doi.org/10.1007/s12672-025-02667-0

[15] YANG H, GONG C, WU Y, XIE X, CHEN Y et al. LncRNA SNHG1 facilitates colorectal cancer cells metastasis by recruiting HNRNPD protein to stabilize SERPINA3 mRNA. Cancer Lett 2024; 604: 217217. https://doi.org/10.1016/j.canlet.2024.217217

[16] SHAN KS, REHMAN TU, IVANOV S, DOMINGO G, RAEZ LE. Molecular Targeting of the BRAF Proto-Oncogene/Mitogen-Activated Protein Kinase (MAPK) Pathway across Cancers. Int J Mol Sci 2024; 25: 624. https://doi.org/10.3390/ijms25010624

[17] VALCIKOVA B, VADOVICOVA N, SMOLKOVA K, ZACPALOVA M, KREJCI P et al. eIF4F controls ERK MAPK signaling in melanomas with BRAF and NRAS mutations. Proc Natl Acad Sci U S A 2024; 121: e2321305121. https://doi.org/10.1073/pnas.2321305121

[18] SARG NH, ZAHER DM, ABU JAYAB NN, MOSTAFA SH, ISMAIL HH et al. The interplay of p38 MAPK signaling and mitochondrial metabolism, a dynamic target in cancer and pathological contexts. Biochem Pharmacol 2024; 225: 116307. https://doi.org/10.1016/j.bcp.2024.116307

[19] LI Y, LI Y, XIANG B, TIAN X, SHI Q et al. IL-2 Combined with IL-15 Enhanced the Expression of NKG2D Receptor on Patient Autologous NK Cells to Inhibit Wilms' Tumor via MAPK Signaling Pathway. J Oncol 2022; 2022: 4544773. https://doi.org/10.1155/2022/4544773

[20] KURTZEBORN K, KWON HN, KUURE S. MAPK/ERK Signaling in Regulation of Renal Differentiation. Int J Mol Sci 2019; 20: 1779. https://doi.org/10.3390/ijms20071779

[21] YAN W, WANG X, WANG W, GUO Q, HUANG N et al. The p38/MAPK pathway as a therapeutic target to prevent therapeutic escape of breast cancer stem cells. Sci China Life Sci 2024; 67: 1867-1880. https://doi.org/10.1007/s11427-023-2585-5

[22] LIU YC, LIN TJ, CHONG KY, CHEN GY, KUO CY et al. Targeting the ERK1/2 and p38 MAPK pathways attenuates Golgi tethering factor golgin-97 depletion-induced cancer progression in breast cancer. Cell Commun Signal 2025; 23: 22. https://doi.org/10.1186/s12964-024-02010-0

[23] GUO F, LING G, QIU J, LI J, GAN Y et al. Juglone induces ferroptosis in glioblastoma cells by inhibiting the Nrf2-GPX4 axis through the phosphorylation of p38MAPK. Chin Med 2024; 19: 52. https://doi.org/10.1186/s13020-024-00920-2

[24] SILVENTE BERNAL S, GIRÓN VALLEJO O, SÁNCHEZ SÁNCHEZ A, MENACHO HERNÁNDEZ C, RODÓN BERRÍO J et al. Late effects of Wilms' tumor treatment. Cir Pediatr 2024; 37: 116-122. https://doi.org/10.54847/cp.2024.03.13

[25] LOW YH, ASI Y, FOTI SC, LASHLEY T. Heterogeneous Nuclear Ribonucleoproteins: Implications in Neurological Diseases. Mol Neurobiol 2021; 58: 631-646. https://doi.org/10.1007/s12035-020-02137-4

[26] YU S, RUAN X, LIU X, ZHANG F, WANG D et al. HNRNPD interacts with ZHX2 regulating the vasculogenic mimicry formation of glioma cells via linc00707/miR-651-3p/SP2 axis. Cell Death Dis 2021; 12: 153. https://doi.org/10.1038/s41419-021-03432-1

[27] WANG Z, HAN H, ZHANG C, WU C, DI J et al. Copy number amplification-induced overexpression of lncRNA LOC101927668 facilitates colorectal cancer progression by recruiting hnRNPD to disrupt RBM47/p53/p21 signaling. J Exp Clin Cancer Res 2024; 43: 274. https://doi.org/10.1186/s13046-024-03193-7

[28] GOUBLE A, GRAZIDE S, MEGGETTO F, MERCIER P, DELSOL G et al. A new player in oncogenesis: AUF1/hnRNPD overexpression leads to tumorigenesis in transgenic mice. Cancer Res 2002; 62: 1489-1495.

[29] LU X, ZHONG J, LIU L, ZHANG W, ZHAO S et al. The function and regulatory mechanism of RNA-binding proteins in breast cancer and their future clinical treatment prospects. Front Oncol 2022; 12: 929037. https://doi.org/10.3389/fonc.2022.929037

[30] ALIMIRAH F, PULIDO T, VALDOVINOS A, ALPTEKIN S, CHANG E et al. Cellular Senescence Promotes Skin Carcinogenesis through p38MAPK and p44/42MAPK Signaling. Cancer Res 2020; 80: 3606-3619. https://doi.org/10.1158/0008-5472.can-20-0108

[31] WANG XF, ZHOU QM, DU J, ZHANG H, LU YY et al. Baicalin suppresses migration, invasion and metastasis of breast cancer via p38MAPK signaling pathway. Anticancer Agents Med Chem 2013; 13: 923-931. https://doi.org/10.2174/18715206113139990143
[32] O'CONNELL CE, VASSILEV A. Combined Inhibition of p38MAPK and PIKfyve Synergistically Disrupts Autophagy to Selectively Target Cancer Cells. Cancer Res 2021; 81: 2903-2917. https://doi.org/10.1158/0008-5472.can-20-3371
[33] LI G, LIAO M, BAO H, XU H, WANG J et al. RNA-binding protein hnRNPD induces epithelial-mesenchymal transition in Wilms' tumor via facilitating MAP4K4 mRNA stability. Mol Genet Genomics 2026; 301: 130. https://doi.org/10.1007/s00438-026-02446-8

Figure Legends

Figure 1. hnRNPD is highly expressed in WT. A) The expression level of hnRNPD in WT was analyzed based on gene expression profiles from the TARGET-WT and GEO138869 datasets. B, C) The mRNA and protein expression levels of hnRNPD in HK-2, 17.94, and HFWT cells were detected using qRT-PCR and Western blot analyses. $^{**}p < 0.01$, $^{***}p < 0.001$, $^{****}p < 0.0001$ vs. Normal tissues or HK-2 cells

Figure 2. Specifically interfere with the expression of hnRNPD in WT cells. A, B) The si-hnRNPD interference plasmid was transfected into 17.94 and HFWT cells, and the mRNA and protein expression levels of hnRNPD were assessed using qRT-PCR and Western blot analyses. $^{**}p < 0.01$, $^{***}p < 0.001$ vs. si-NC group

Figure 3. The effects of silencing hnRNPD on proliferation and apoptosis. A) CCK-8 assay was used to assess the viability of 17.94 and HFWT cells at 12, 24, 48, and 72 h. B) EdU staining was performed to evaluate proliferation of 17.94 and HFWT cells. C) Flow cytometry was employed to analyze apoptosis rates of 17.94 and HFWT cells. D) Western blot analysis was conducted to determine the protein expression levels of PCNA, Cyclin D1, and Cleaved Caspase-3 in 17.94 and HFWT cells. $^{*}p < 0.05$, $^{**}p < 0.01$, $^{***}p < 0.001$ vs. si-NC group

Figure 4. Silencing hnRNPD inhibits the activation of the p38 signaling pathway in WT cells. A) Based on the WT-related gene expression profiles from the TARGET-WT dataset, 241 genes associated with hnRNPD were identified and a network diagram was constructed. B) Seventeen core genes were identified based on centrality score analysis. C) Western blot analysis was employed to assess the phosphorylation levels of p38 MAPK in HK-2 cells, as well as in 17.94 and HFWT cells transfected with si-hnRNPD. $^{***}p < 0.001$ vs. HK-2 cells. $^{\#}p < 0.05$, $^{\#\#}p < 0.01$ vs. si-NC group

Figure 5. Inhibition of p38 MAPK activation reverses the promoting effect of hnRNPD on the malignant proliferation of WT cells. A, B) Following transfection of the hnRNPD overexpression plasmid into 17.94 and HFWT cells, the mRNA and protein expression levels of hnRNPD were assessed via qRT-PCR and Western blot analyses. C) CCK-8 assay was used to assess the viability of 17.94 and HFWT cells. D) EdU staining was performed to evaluate proliferation of 17.94 and HFWT cells. Bar scale=50 μm. *p < 0.05, **p < 0.01, ***p < 0.001 vs. Vector group. #p < 0.05, ##p < 0.01, ###p < 0.001 vs. Oe-hnRNPD group

Figure 6. Inhibition of p38 MAPK activation reverses the inhibitory effect of hnRNPD on apoptosis of WT cells. A) Flow cytometry was employed to analyze apoptosis rate of 17.94 and HFWT cells. B) Western blot analysis was conducted to determine the protein expression levels of PCNA, Cyclin D1, and Cleaved Caspase-3 in 17.94 and HFWT cells. *p < 0.05, **p < 0.01, ***p <0.001 vs. Vector group. #p < 0.05, ##p < 0.01, ###p < 0.001 vs. Oe-hnRNPD group

Fig. 1 Download full resolution image

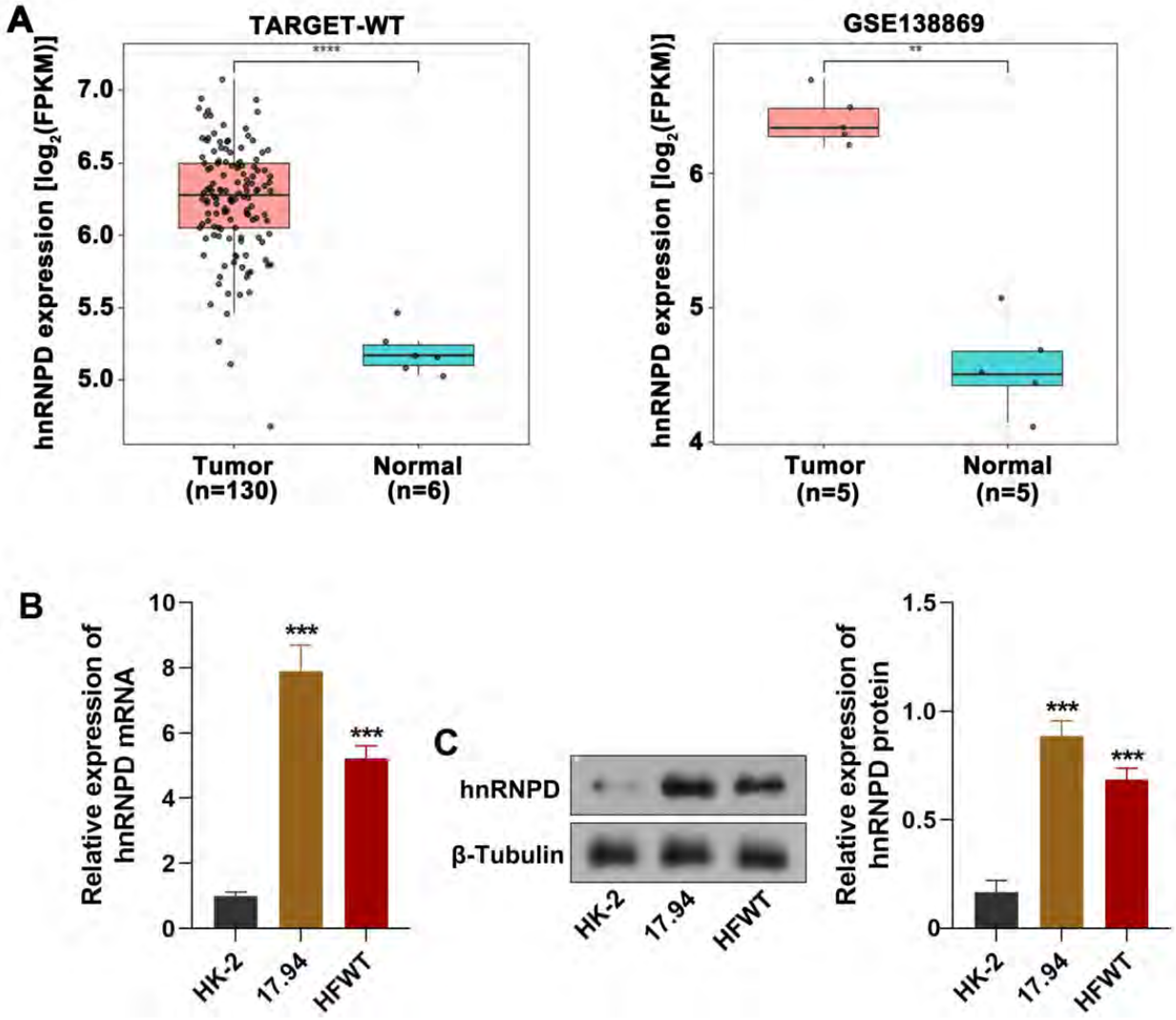

Fig. 2 Download full resolution image

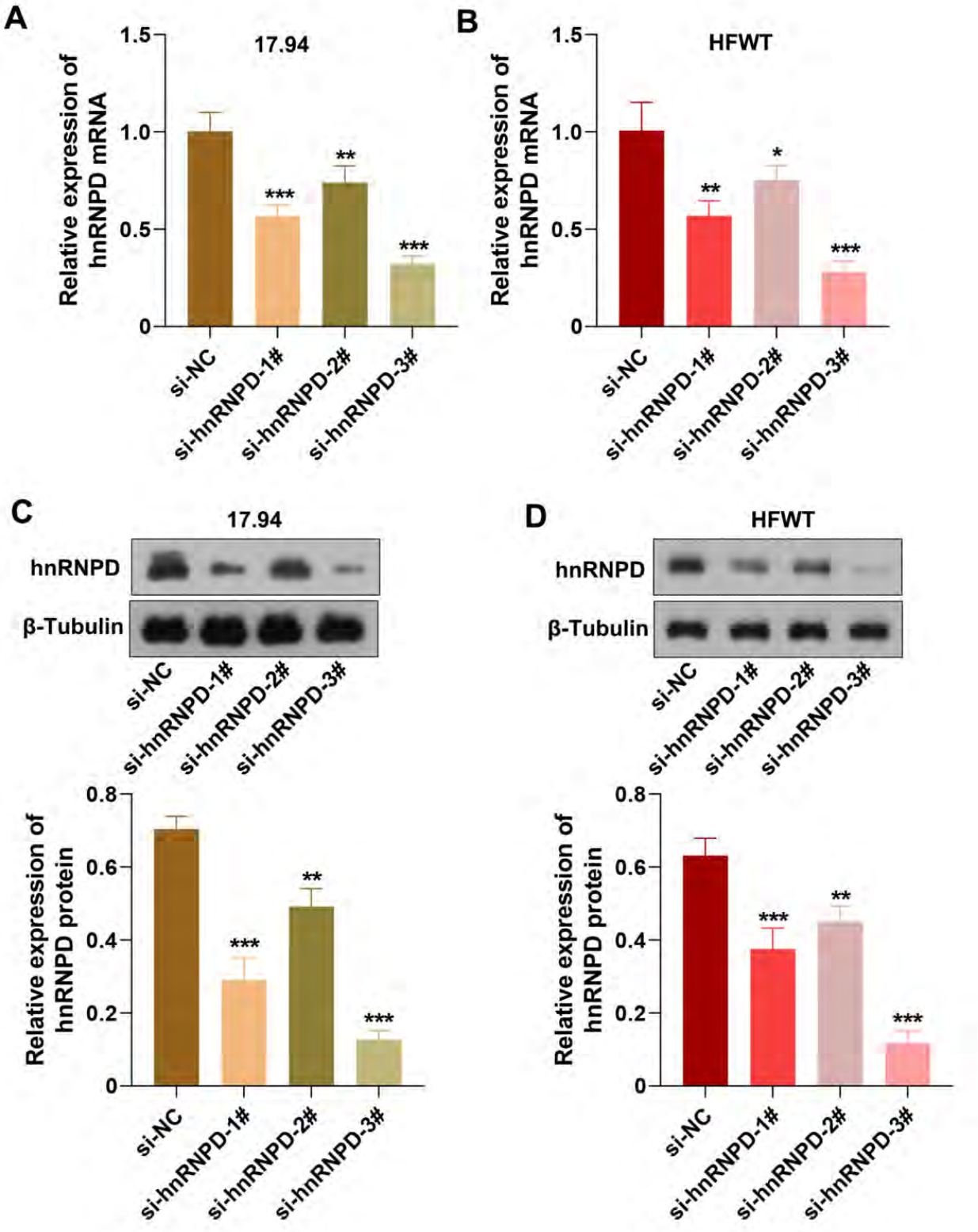

Fig. 3 [Download full resolution image]

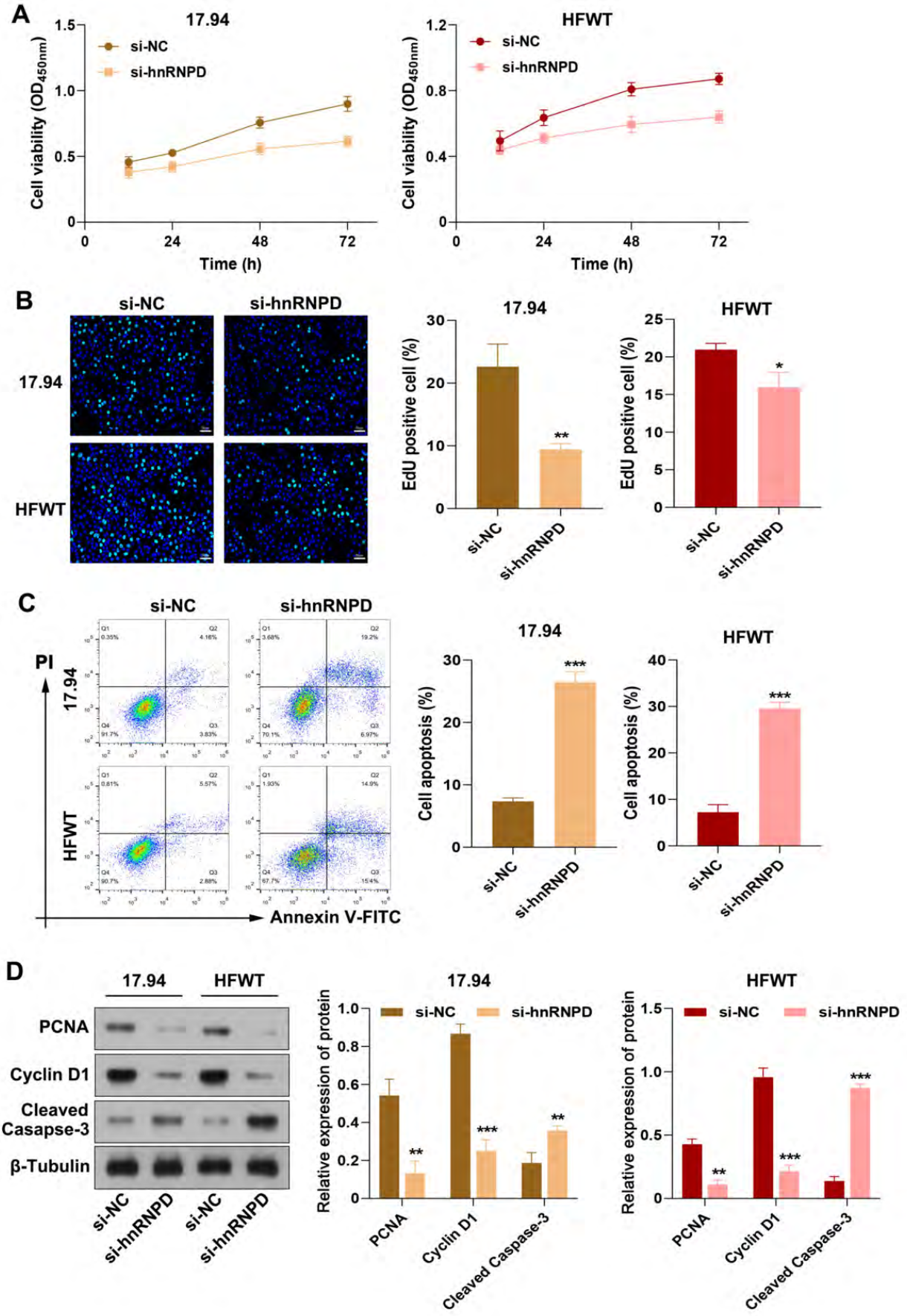

Fig. 4 Download full resolution image

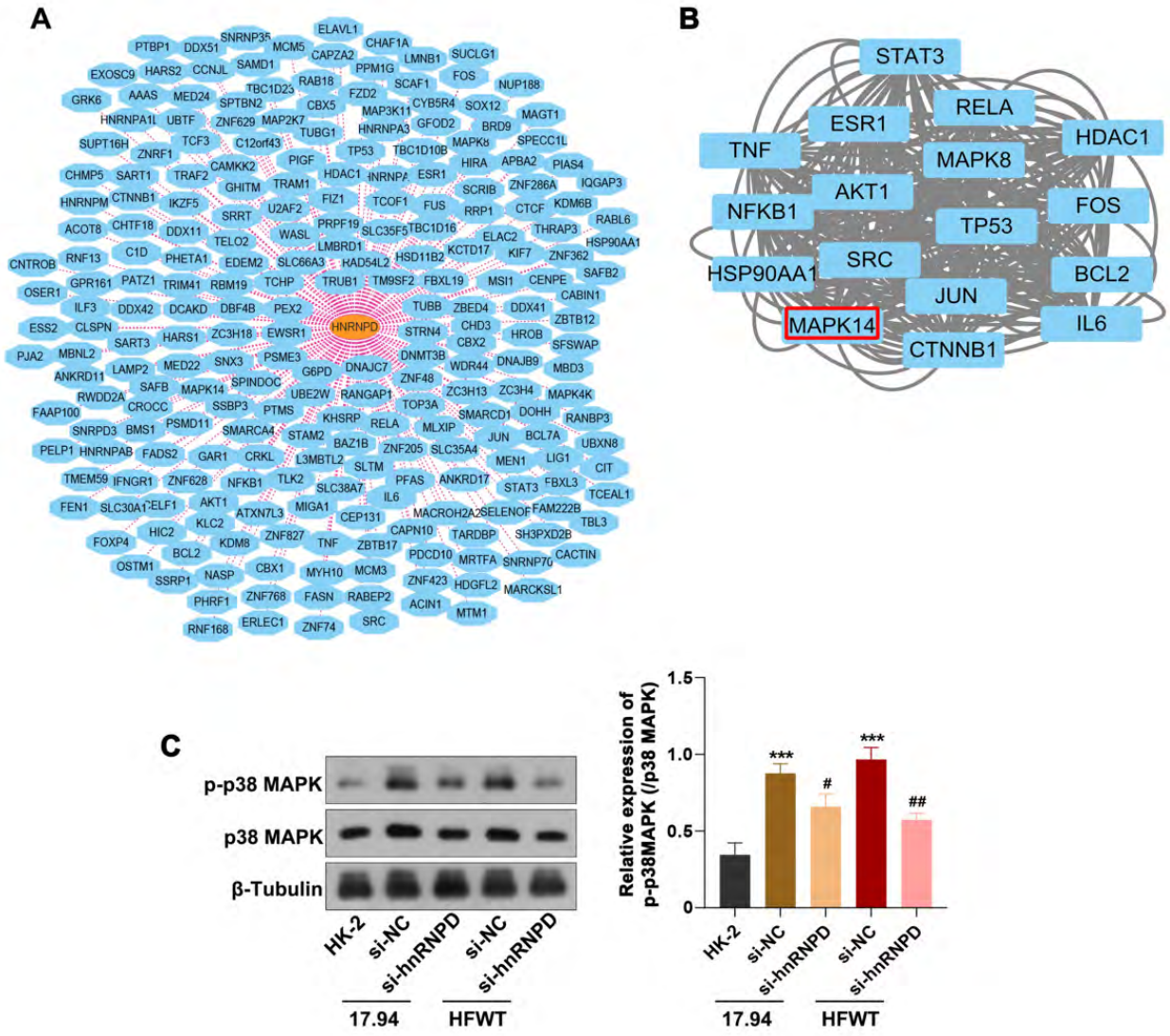

Fig. 5 Download full resolution image

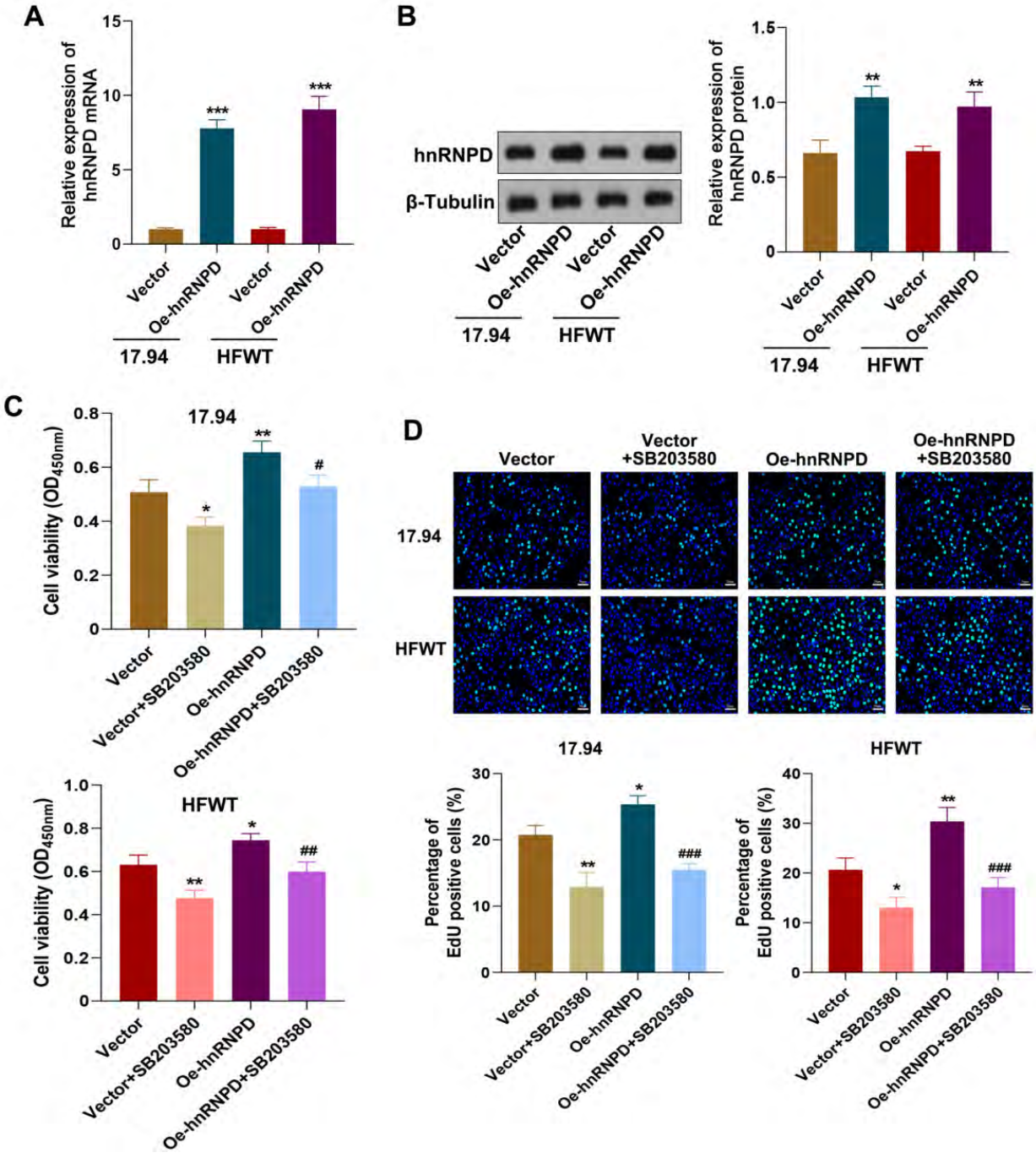

Fig. 6 Download full resolution image